HNPS Advances in Nuclear Physics

Vol 24 (2016)

HNPS2016

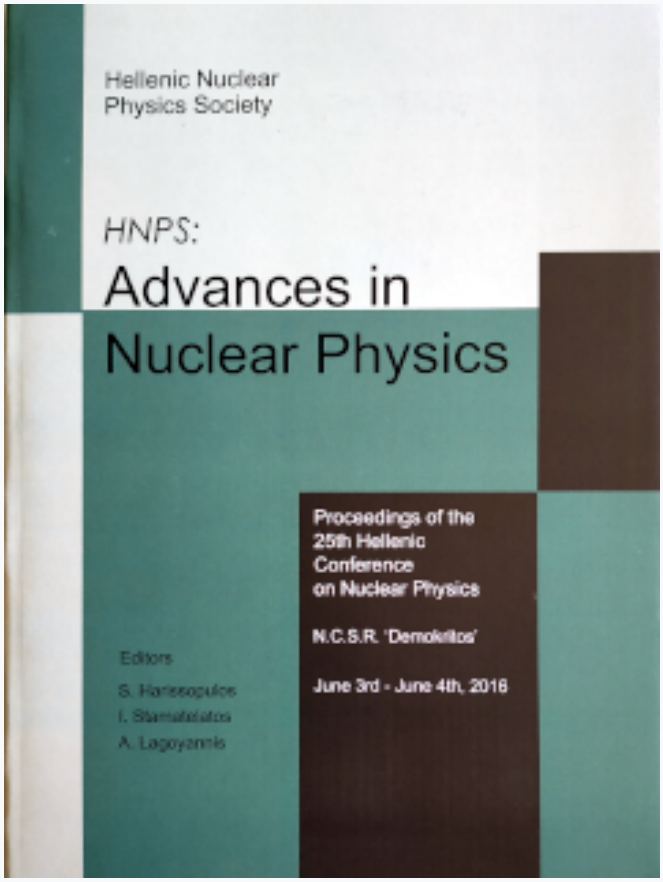

The 240Pu(n,f) cross section measurement at the new experimental area at CERN's n_TOF facility

A. Stamatopoulos, for the nTOF Collaboration

doi: 10.12681/hnps.1857

The ^{240}Pu(n,f) cross section measurement at the new experimental area at CERN's n_TOF facility

A. Stamatopoulos[1,*], A. Tsinganis[1,2], N. Colonna[3], R. Vlastou[1], M. Kokkoris[1], P. Schillebeeckx[4], A. Plompen[4], J. Heyse[4], P. Žugec[6], M. Barbagallo[3], M. Calviani[2], E. Berthoumieux[5], E. Chiaveri[2], O. Aberle[2], J. Andrzejewski[7], L. Audouin[8], V. Bécares[9], M. Bacak[10], J. Balibrea[9], S. Barros[11], F. Beˇcvárˇ[12], C. Beinrucker[13], F. Belloni[5], J. Billowes[14], V. Boccone, D. Bosnar[6], M. Brugger[2], M. Caamaño[15], F. Calviño[16], D. Cano-Ott[9], F. Cerutti[2], G. Cortés[16], M. A. Cortés-Giraldo[17], L. Cosentino[18], L. A. Damone[4,19], K. Deo[20], M. Diakaki[5,1], C. Domingo-Pardo[21], R. Dressler[22], E. Dupont[5], I. Durán[15], B. Fernández-Domínguez[15], A. Ferrari[2], P. Ferreira[11], P. Finocchiaro[19], R. J. W. Frost[14], V. Furman[23], K. Göbel[13], M. B. Gómez-Hornillos[16], A. R. García[9], I. Gheorghe[24], T. Glodariu[24], I. F. Gonçalves[11], E. González[9], A. Goverdovski[25], E. Griesmayer[10], C. Guerrero[17], F. Gunsing[5,2], H. Harada[26], T. Heftrich[13], S. Heinitz[22], A. Hernández-Prieto[2,16], D. G. Jenkins[27], E. Jericha[10], F. Käppeler[28], Y. Kadi[2], T. Katabuchi[29], P. Kavrigin[10], V. Ketlerov[25], V. Khryachkov[25], A. Kimura[26], N. Kivel[22], M. Krtiˇcka[12], E. Leal-Cidoncha[15], C. Lederer[13,30], H. Leeb[10], J. Lerendegui-Marco[17], M. Licata[31,32], S. Lo Meo[31,33], R. Losito[2], D. Macina[2], J. Marganiec[2], T. Martínez[9], C. Massimi[31,32], P. Mastinu[34], M. Mastromarco[3], F. Matteucci[35,36], E. Mendoza[9], A. Mengoni[33], P. M. Milazzo[35], F. Mingrone[31], M. Mirea[24], S. Montesano[2], A. Musumarra[18,37], R. Nolte[38], F. R. Palomo-Pinto[17], C. Paradela[15], N. Patronis[39], A. Pavlik[40], J. Perkowski[7], J. I. Porras[2,41], J. Praena[17], J. M. Quesada[17], T. Rauscher[42,43], R. Reifarth[13], A. Riego-Perez[16], M. Robles[15], C. Rubbia[2], J. A. Ryan[14], M. Sabaté-Gilarte[2,17], A. Saxena[20], S. Schmidt[13], D. Schumann[22], P. Sedyshev[23], A. G. Smith[14], S. V. Suryanarayana[20], G. Tagliente[3], J. L. Tain[21], A. Tarifeño-Saldivia[21], L. Tassan-Got[8], S. Valenta[12], G. Vannini[31,32], V. Variale[3], P. Vaz[11], A. Ventura[31], V. Vlachoudis[2], A. Wallner[44], S. Warren[14], M. Weigand[13], C. Weiss[2,10] and T. Wright[14]

1 National Technical University of Athens (NTUA), Greece
2 European Organisation for Nuclear Research (CERN), Geneva, Switzerland
3 Istituto Nazionale di Fisica Nucleare, Sezione di Bari, Italy
4 European Commission JRC, Institute for Reference Materials and Measurements, Retieseweg 111, B-2440 Geel, Belgium
5 Commissariat à l'Énergie Atomique (CEA) Saclay - Irfu, Gif-sur-Yvette, France
6 Department of Physics, Faculty of Science, University of Zagreb, Croatia
7 University of Lodz, Poland
8 Institut de Physique Nucléaire, CNRS-IN2P3, Univ. Paris-Sud, Université Paris-Saclay, F-91406 Orsay Cedex, France
9 Centro de Investigaciones Energeticas Medioambientales y Tecnológicas (CIEMAT), Spain
10 Technische Universität Wien, Austria
11 Instituto Superior Técnico, Lisbon, Portugal
12 Charles University, Prague, Czech Republic
13 Goethe University Frankfurt, Germany
14 University of Manchester, United Kingdom
15 University of Santiago de Compostela, Spain
16 Universitat Politècnica de Catalunya, Spain
17 Universidad de Sevilla, Spain
18 INFN Laboratori Nazionali del Sud, Catania, Italy
19 Dipartimento di Fisica, Università degli Studi di Bari, Italy
20 Bhabha Atomic Research Centre (BARC), India
21 Instituto de Física Corpuscular, Universidad de Valencia, Spain
22 Paul Scherrer Institut (PSI), Villingen, Switzerland
23 Joint Institute for Nuclear Research (JINR), Dubna, Russia
24 Horia Hulubei National Institute of Physics and Nuclear Engineering, Romania
25 Institute of Physics and Power Engineering (IPPE), Obninsk, Russia

26 Japan Atomic Energy Agency (JAEA), Tokai-mura, Japan
27 University of York, United Kingdom
28 Karlsruhe Institute of Technology, Campus North, IKP, 76021 Karlsruhe, Germany
29 Tokyo Institute of Technology, Japan
30 School of Physics and Astronomy, University of Edinburgh, United Kingdom
31 Istituto Nazionale di Fisica Nucleare, Sezione di Bologna, Italy
32 Dipartimento di Fisica e Astronomia, Università di Bologna, Italy
33 Agenzia nazionale per le nuove tecnologie (ENEA), Bologna, Italy
34 Istituto Nazionale di Fisica Nucleare, Sezione di Legnaro, Italy
35 Istituto Nazionale di Fisica Nucleare, Sezione di Trieste, Italy
36 Dipartimento di Astronomia, Università di Trieste, Italy
37 Dipartimento di Fisica e Astronomia, Università di Catania, Italy
38 Physikalisch-Technische Bundesanstalt (PTB), Bundesallee 100, 38116 Braunschweig, Germany
39 University of Ioannina, Greece
40 University of Vienna, Faculty of Physics, Vienna, Austria
41 University of Granada, Spain
42 Centre for Astrophysics Research, University of Hertfordshire, United Kingdom
43 Department of Physics, University of Basel, Switzerland
44 Australian National University, Canberra, Australia

Abstract The accurate knowledge of the neutron-induced fission cross-sections of actinides and other isotopes involved in the nuclear fuel cycle are essential for the design of advanced nuclear systems. These experimental data can also provide feedback for the adjustment of nuclear model parameters used in the evaluation process, resulting in further developments of nuclear fission models. In the present work, the ^{240}Pu(n,f) cross-section was measured at CERN's n_TOF facility over a wide range of neutron energies, from a few meV to several MeV, using the time-of-flight technique and a set-up based on MicroMegas detectors. This measurement was the first experiment to be performed in n_TOF's new experimental area (EAR-2), which offers a significantly higher neutron flux compared to the existing experimental area. Preliminary results as well as the experimental procedure, including a brief description of the facility, the sample mounting, the read-out process and the data handling and analysis, are presented.

Keywords Fission, ^{240}Pu, Micromegas, n_TOF,/CERN Cross Section

---

INTRODUCTION

The development and optimum design of advanced nuclear systems, such as Generation-IV nuclear reactors and Accelerator Driven Systems, requires the accurate knowledge of neutron induced fission cross sections of plutonium isotopes and other minor actinides [1, 2]. More specifically, the ^{240}Pu isotope is included in the Nuclear Energy Agency's (NEA) High Priority Request List (HPRL) [3] as well as in the NEMEA-4 meeting proceedings [4]. Requested target accuracies are in the order of 1.6% − 11.8% for the energy region 0.454 keV − 6.07 MeV compared to the presently reported 3.9% − 21.6%. The previous measurement of the ^{240}Pu(n,f) cross section carried out at the n-TOF's Experimental Area 1 (EAR-1), was unsuccessful due to detector deterioration caused by the high alpha activity of the ^{240}Pu

samples in addition to the long period in time, needed to complete the measurement [5], therefore it had to be remeasured in the newly commissioned experimental area EAR-2, which offers a significantly higher instantaneous neutron flux and a higher background suppression thus reducing the time needed to complete the measurement. Similar recent measurements have also been performed at GNEIS[6], LANSCE [7] and IRMM [8].

EXPERIMENTAL SETUP

The n_TOF Facility

The measurement was performed at CERN's n_TOF facility [9–11], in the newly commissioned experimental area EAR-2 [12]. The white neutron spectrum, which is produced by spallation, occurring when a 20 GeV/c pulsed proton beam, delivered by CERN's Proton Synchrotron [13], impinges on a 40 cm in length and 60 cm in diameter lead block, spans from the meV to the GeV energy region.The proton pulse has a duration of 6 ns RMS, a maximum repetition rate of 1 pulse per 1.2 s and nominally carries 7×10^{12} protons. The 1.3 ton lead target is surrounded by a 1 cm-thick layer of demineralized water and only in the upstream direction an additional 4 cm-thick layer of borated water in saturation, (H_20 + 1.28% H_3BO_3 , fraction in mass) which act as coolant and neutron moderator respectively. Following the target in the beam direction, a beam pipe of 182.3 m leads to the first experimental area EAR-1. The new experimental area EAR-2 is located 18.16 m above the spallation target, perpendicular to the beam direction, offering a 25 − 30 times higher flux [14] and approximately 10 times shorter time of flights compared to the existing area. The high instantaneous flux, combined with the wide white neutron spectrum (from thermal energies to the MeV region), leads to the relative suppression of the contribution originating from the high intrinsic α−background of the samples, thus allowing for accurate measurements below the fission threshold, where the fission cross section is low.

Samples

Three high purity (99.89%) plutonium dioxide (PuO_2) samples, prepared at JRC-Geel (Belgium) [15] for the previous measurement in EAR-1, were used having a total ^{240}Pu mass of 2.288 mg ($\sim$ 100μgr/cm^2 per sample) and a total α-activity of 19.219 MBq. The oxide material was electro-deposited on a 250 μm-thick aluminum backing with a diameter of 5 cm, while the deposit itself had a diameter of 3 cm. In addition to the plutonium samples, two targets were used as reference : a ^{235}U and a ^{238}U, with a mass of $\sim$ 0.6 mg and $\sim$ 0.8 mg respectively. The impurities found in the samples, mainly ^{239}Pu, have a non negligible contribution in the obtained yields below 1 keV, which was thoroughly taken into account in the analysis.

Detectors

The measurement was carried out using a set-up based on the compact and low-mass Micromegas (Micro-Mesh Gaseous Structure) gaseous detector [16–18]. Its main volume is divided into two parts by a thin, 35 μm pitched micro-mesh : a drift region (5 mm) and a

narrow amplification region (50 μm), in which a high electric field causes an avalanche multiplication. Typical operating electric fields are ~1 kV/cm and ~100 kV/cm respectively mainly depending on the dielectric strength of the gas used, which in this case was a mixture of Ar : CF_4 : $isoC_4H_{10}$ (88:10:2) at slightly atmospheric overpressure and room temperature. The detector set-up consisted of 6 similar detectors in total (3 for the plutonimum samples, 2 for the uranium samples and 1 for monitoring possible proton recoils from the surrounding materials), all of which were housed in a cylindrical aluminum chamber as shown in figure 1.

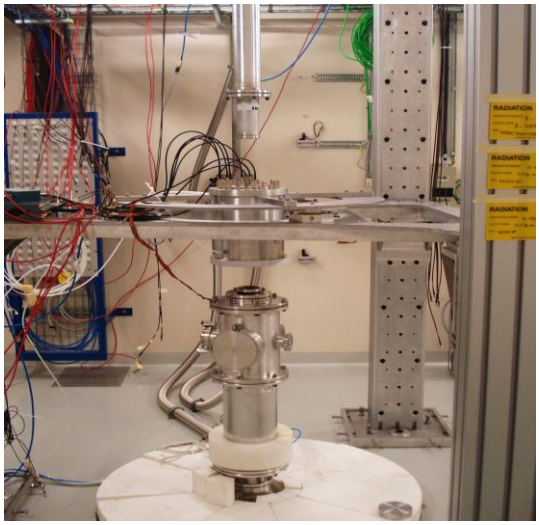

Fig. 1. The fission chamber, which housed the detectors and samples, as seen inside the experimental area EAR-2, during the measurement, in the middle of the picture. The neutron beam was delivered vertically from bottom to top.

DATA ANALYSIS

An offline pulse shape analysis routine [19] parses the raw data, determining, among others, the amplitude and the position in time of every recorded signal. During the experiment, beam-off data was obtained in order to measure the contribution of the α-activity as well as spontaneous fission.

As mentioned before, the impurities found in the sample were treated separately by calculating the product of the fission cross section, as found in ENDF/B-VII evaluations, and the atomic abundance of each individual plutonium isotope, as a function of energy. The aforementioned product can be seen in fig. 2 and is commonly referred to in the literature as weighted cross section. The contribution of the impurities in the energy point wise experimental counting spectrum can be derived as the fraction of the sum of the contaminants's weighted cross section over the sum of the isotopes's weighted cross sections found in the sample, including the one from ^{240}Pu.

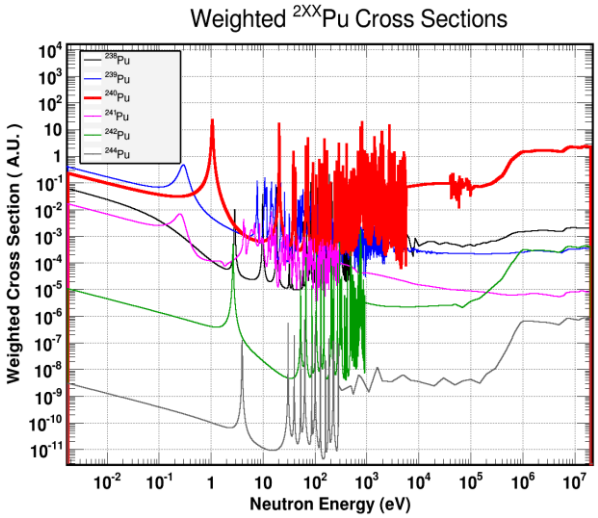

Fig. 2. The calculated weighted cross sections for ^{240}Pu and the contaminants found in the samples. It is evident that bellow 100 eV the main contaminant that contributes to the experimental yield is ^{239}Pu.

The ^{240}Pu(n,f) cross section was calculated using the reference reactions ^{235}U(n,f) and ^{238}U(n,f) for flux normalization purposes. The detector dead time, as well as the background contribution due to sample impurities were taken into account during the analysis. The final experimental cross section was derived from the weighted average between the three individual cross sections, calculated for each plutonium target. Preliminary results are shown in figure 3 for the energy range 6 keV − 35 keV, while resonances can be resolved up to a few tens of keV. The present preliminary data comparison with the latest ENDF/B-VII.1 library [20], reveals that the aforementioned resonances are not included in the evaluations, as figure 3 demonstrates. Resonance analysis is planned to be performed, using R-matrix calculations, to characterize the resolved resonances.

CONCLUSIONS

The ^{240}Pu neutron induced fission cross section, is the first measurement to be performed in the newly commissioned experimental area EAR-2, at CERN's n_TOF facility. Data was obtained over a wide energy range that spans from thermal energies up to at least a few MeV. Most remarkably, data in the sub-threshold region, shows clear resonance structures which are not included in the evaluated libraries. R-matrix calculations will be performed to characterize these structures. In the MeV region, preliminary data shows a general agreement with the evaluations, yet further analysis is ongoing. The higher instantaneous flux along with the stronger background suppression, compared to the existing experimental area EAR-1, are deemed crucial to the success of this measurement, following which additional measurements are planned that include the study of short-lived isotopes.

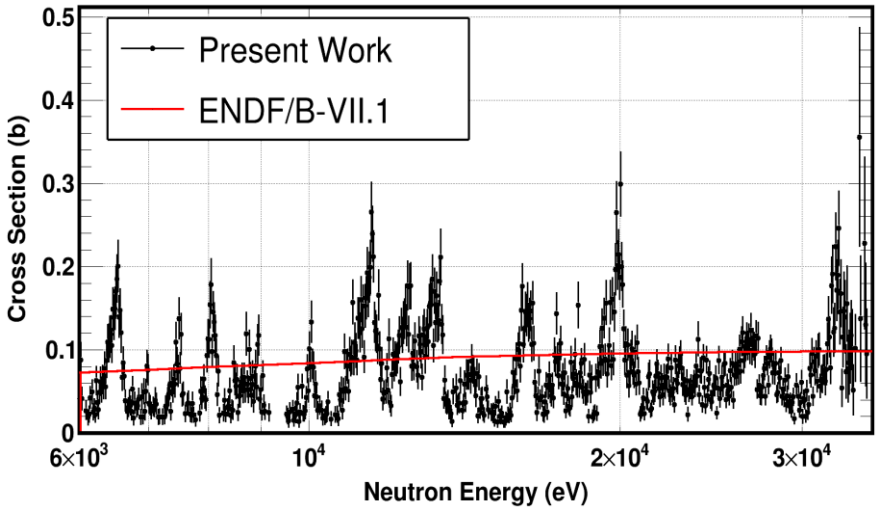

Fig. 3. Comparison between present data (black points) and ENDF/B-VII.1 evaluation (red line) in the energy range 6 keV − 35 keV. Clusters of resonances, that are attributed to transitions between Class-I and Class-II states are visible, while resonances can be resolved up to a few tens of keV. Data is shown using a binning of 2000 bins per energy decade.

References

[1] https://www.gen-4.org/gif/jcms/c_9260/public/
[2] https://www.ifnec.org/ifnec/
[3] https://www.oecd-nea.org/dbdata/hprl/hprl.pl
[4] M. Salvatores et al, NEMEA-4 proceedings, JRC 42917
[5] A. Tsinganis et al., Deliverable 1.5 of the ANDES project, Ch. 3, JRC85144 (2013)
[6] A. B. Laptev et al., Nuclear Physics A 734, p. E45 – E48 (2004)
[7] F. Tovesson et al., Physical Review C 79, p. 014613 (2009)
[8] P. Salvador-Castiñeira et al., Physics Procedia 64, p. 177 - 182 (2015)
[9] U. Abbondanno et al., CERN-SL-2002-053 ECT
[10] C. Guerrero et al., Eur. Phys. J. A 49, p. 1-15 (2013)
[11] E. Berthoumieux et al., CERN-nTOF-PUB-2013-001
[12] C. Weiß et al., NIM A 799, p. 90-98 (2015)
[13] J.P. Burnet et al., CERN-2011-004, 2011
[14] A. Tsinganis et al., 14th International Conference on Nuclear Reaction Mechanisms Proceedings, p. 21-26 (2016)
[15] G. Sibbens et al., J. Radioanal. Nucl. Ch. 299, p. 1093-1098(2014)
[16] Y. Giomataris et al., NIM A 376 (1), p. 29 – 35 (1996)
[17] Y. Giomataris, NIM A 419, p. 230 – 250 (1998)
[18] Y. Giomataris, ICFA Instrum. Bul.19
[19] P. Žugec et al., NIM A 812, p. 134 - 144 (2016)
[20] https://www-nds.iaea.org/exfor/endf.htm